Peritumoral imaging features of thymic epithelial tumors for the prediction of transcapsular invasion: beyond intratumoral analysis

Jongmin Park*
Byunggeon Park*
Jihoon Hong
Jung Guen Cha
Kyung Min Shin
Jaehee Lee
An Na Seo
Young Woo Do
Won Kee Lee
Jae-Kwang Lim

*These authors contributed equally to this work.

PURPOSE

The purpose of this study was to differentiate cases without transcapsular invasion (Masaoka–Koga stage I) from cases with transcapsular invasion (Masaoka–Koga stage II or higher) in patients with thymic epithelial tumors (TETs) using tumoral and peritumoral computed tomography (CT) features.

METHODS

This retrospective study included 116 patients with pathological diagnoses of TETs. Two radiologists evaluated clinical variables and CT features, including size, shape, capsule integrity, presence of calcification, internal necrosis, heterogeneous enhancement, pleural effusion, pericardial effusion, and vascularity grade. Vascularity grade was defined as the extent of peritumoral vascular structures in the anterior mediastinum. The factors associated with transcapsular invasion were analyzed using multivariable logistic regression. In addition, the interobserver agreement for CT features was assessed using Cohen's or weighted kappa coefficients. The difference between the transcapsular invasion group and that without transcapsular invasion was evaluated statistically using the Student's t-test, Mann–Whitney U test, chi-square test, and Fisher's exact test.

RESULTS

Based on pathology reports, 37 TET cases without and 79 with transcapsular invasion were identified. Lobular or irregular shape [odds ratio (OR): 4.19; 95% confidence interval (CI): 1.53–12.09; $P = 0.006$], partial complete capsule integrity (OR: 5.03; 95% CI: 1.85–15.13; $P = 0.002$), and vascularity grade 2 (OR: 10.09; 95% CI: 2.59–45.48; $P = 0.001$) were significantly associated with transcapsular invasion. The interobserver agreement for shape classification, capsule integrity, and vascularity grade was 0.840, 0.526, and 0.752, respectively ($P < 0.001$ for all).

CONCLUSION

Shape, capsule integrity, and vascularity grade were independently associated with transcapsular invasion of TETs. Furthermore, three CT TET features demonstrated good reproducibility and help differentiate between TET cases with and without transcapsular invasion.

KEYWORDS

Cancer, computed tomography, thymic epithelial tumor, thymoma, tumor

From the Department of Radiology (J.P., J.H., J.G.C., J-K.L. ✉ limjk@knu.ac.kr), School of Medicine, Kyungpook National University, Daegu, South Korea; Department of Radiology (B.P., K.M.S.), School of Medicine, Kyungpook National University, Kyungpook National University Chilgok Hospital, Daegu, South Korea; Department of Internal Medicine (J.L.), School of Medicine, Kyungpook National University, Daegu, South Korea; Department of Pathology (A.N.S.), School of Medicine, Kyungpook National University, Kyungpook National University Chilgok Hospital, Daegu, South Korea; Department of Thoracic and Cardiovascular Surgery (Y.W.D.), School of Medicine, Kyungpook National University, Daegu, South Korea; Medical Research Collaboration Center in Kyungpook National University Hospital (W.K.L.), School of Medicine, Kyungpook National University, Daegu, South Korea.

Thymic epithelial tumors (TETs), originating in thymic epithelial cells, are rare tumors of the anterior (prevascular) mediastinum, with a reported annual incidence ranging from 1.3 to 3.2 per million globally.[1,2] Histologically, various staging systems have been proposed for TETs, including the tumor, nodes, and metastases (TNM) classification of malignant tumors and non-TNM based staging systems.[3] The Masaoka–Koga staging system has been extensively used to classify and stage TETs, including thymomas and thymic carcinomas, based on the extent of tumor invasion.[4,5] In the Masaoka–Koga staging system, the distinction

between stages I and II is based on whether the tumor exhibits transcapsular invasion.[6] Transcapsular invasion is a key factor associated with disease recurrence and patient survival.[7,8] In Masaoka–Koga stages I and II, the 10-year survival rates are 90% and 70% and the average recurrence rates 3% and 11%, respectively.[7] Additionally, prognostic difference can influence the treatment plan for patients with TET.

Enhanced chest computed tomography (CT) is currently the preferred imaging examination for the initial assessment of patients with TET. Although several studies have suggested an association between the Masaoka–Koga staging system and TET CT features, such as tumor size, shape, and internal characteristics, distinguishing between Masaoka–Koga stages I and II remains challenging when using a preoperative chest CT.[9-13] Although pleural effusion, enlarged lymph nodes, and pleural or pulmonary nodules have been assessed in patients with TETs, CT analysis has limited value in the prediction of the Masaoka–Koga stage.[10-14] However, to our knowledge, no studies have analyzed the association between the peritumoral CT features of TETs and the Masaoka–Koga staging system.

Distinguishing between Masaoka–Koga stages I and II preoperatively is crucial for determining an appropriate surgical plan of either complete thymectomy or thymomectomy.[15-17] The aim of this study was to retrospectively investigate the potential factors relating to tumoral and peritumoral CT features that influence transcapsular invasion using preoperative chest CT.

Methods

The institutional review board of the participating hospitals approved this retrospective study, and the requirement for patient consent was waived (KNUH 2021-03-004).

Main points

- The peritumoral computed tomography (CT) features of thymic epithelial tumors (TET) provide additional information for predicting transcapsular invasion.

- The intratumoral and peritumoral CT features of TETs exhibit good reproducibility.

- In patients with TETs, the CT features of shape, capsule integrity, and peritumoral vascularity help differentiate between those with transcapsular invasion and those without.

Study population and computed tomography acquisition

We retrospectively reviewed 132 preoperative chest CT scans of patients diagnosed with TETs between January 2012 and December 2020 from Kyungpook National University Hospital and Kyungpook National University Chilgok Hospital, Daegu, South Korea. Patients who only underwent chest CT at other hospitals were analyzed using the CT images acquired from these hospitals. All patients underwent chest CT scans within 2 weeks prior to surgery. In total, 16 patients were excluded from our study for the following reasons: radiation therapy before surgery (3/16, 18.8%), inappropriate pathology results (1/16, 6.3%), definite signs of seeding or the invasion of adjacent structures such as large vessels (4/16, 25%), surgical biopsy without total tumor resection (2/16, 12.5%), non-enhanced CT scans (4/16, 25%), and poor CT imaging quality (2/16, 12.5%). In total, 116 chest CT images from 116 patients were included in this study, some of which originated from our hospital (n = 57) and the remainder from other hospitals (n = 59). According to the Masaoka–Koga stage, there were 37 (31.9%) patients at stage I, 37 (31.9%) at stage IIa, 27 (23.3%) at stage IIb, 13 (11.2%) at stage III, and 2 (1.7%) at stage IV. All CT scans were performed using multiple multidetector CT scanners, including 16-, 64-, 128-, 192-, and 320-slice scanners. The CT scans were obtained in the supine position at full inspiration using contrast media. Axial and coronal images were reconstructed with a sharp or standard reconstruction kernel. In all patients, the CT examination used slice thicknesses of 1.0–5.0 mm, a slice gap of 1.0–5.0 mm, kVp values in the range of 90–140, CT dose index–volume values in the range of 2.251–62.24, and dose-length product values in the range of 148.1–914. An automatic tube current was used for all patients.

Clinical variables and computed tomography image analysis

The following clinical data of each patient at admission were collected from the medical records: age, sex, and presence of myasthenia gravis. Two radiologists (J.P. and B.P., with 8- and 5-years' experience in thoracic radiology, respectively) independently performed a retrospective assessment of TET chest CT features based on enhanced images, including tumor size, shape, capsule integrity, internal necrosis, presence of calcification, pleural effusion, pericardial effusion, and vascularity grade, without knowledge of

the clinical and pathological results. We also evaluated non-contrast CT images to evaluate the presence of calcification and the heterogeneous enhancement of TETs.

In case of disagreement, final decisions on the TET features on chest CTs were reached by consensus. Tumor size was defined as the longest diameter among the axial and coronal images of the chest CT. Shape was classified as round, oval, lobulated, or irregular, with or without capsule integrity. Capsule integrity was defined as almost complete (smooth or shallow lobulation) and partial complete (deep lobulation or spiculate protuberance).[18,19] Vascularity grade was defined as the extent of peritumoral vascular structures in the anterior mediastinum and was evaluated at the largest distribution of the vascular structure among the axial and coronal images in the mediastinal setting [width, 440 Hounsfield units (HU); level, 45 HU] of the enhanced chest CT based on the use of CT images at magnifications in the range of ×3–4. It was evaluated subjectively using a 3-point grading scale according to the following criteria: 0, no visible peritumoral vascular structure; 1, non-measurable slit-like peritumoral vascular structure; 2, measurable peritumoral hypertrophied vascular structure, with a size >1 mm (Figure 1). Representative cases of TETs are presented in Figure 2.

Pathological analysis

All pathological specimens were formalin fixed, paraffin embedded, and stained with hematoxylin and eosin. All histopathological specimens were classified by two pathologists with more than 10-years' experience in line with the fourth edition of the World Health Organization (WHO) classification and Masaoka–Koga staging system.

Statistical Analysis

Categorical variables were expressed as frequency and percentages (%) and were compared between the two groups using the chi-square or Fisher's exact tests. Continuous variables were tested for normality using the Shapiro–Wilk test. Normally distributed data were presented as mean ± standard deviation and analyzed using the Student's t-test; however, non-normally distributed data were expressed as median and interquartile range (IQR) and analyzed using the Mann–Whitney U test. The odds ratio (OR) and confidence interval (CI) from the multivariable logistic analysis were used to identify factors that were independently
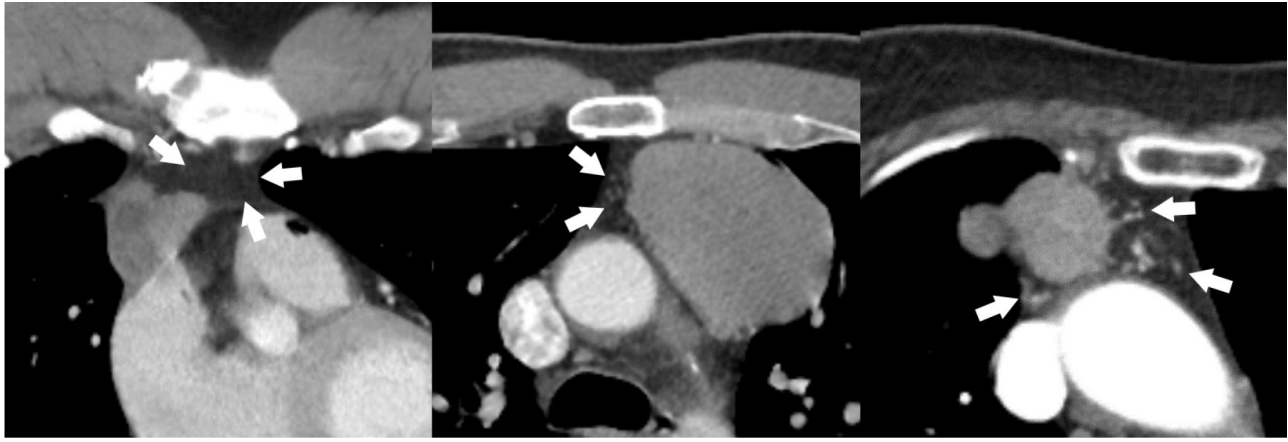
Figure 1. Vascularity grade on representative thymic epithelial tumors (TETs). Vascularity grade was assessed as the extent of peritumoral vascular structures in the anterior mediastinum. Vascularity grade 0 signified no visible vascular structure around the TET in the anterior mediastinum (left image). Vascularity grade 1 was defined as the presence of non-measurable, slit-like vascular structures (arrows) around the TET in the anterior mediastinum (middle image). Vascularity grade 2 was defined as the presence of measurable vascular structures with a size ≥1 mm around the TET in the anterior mediastinum (right image).
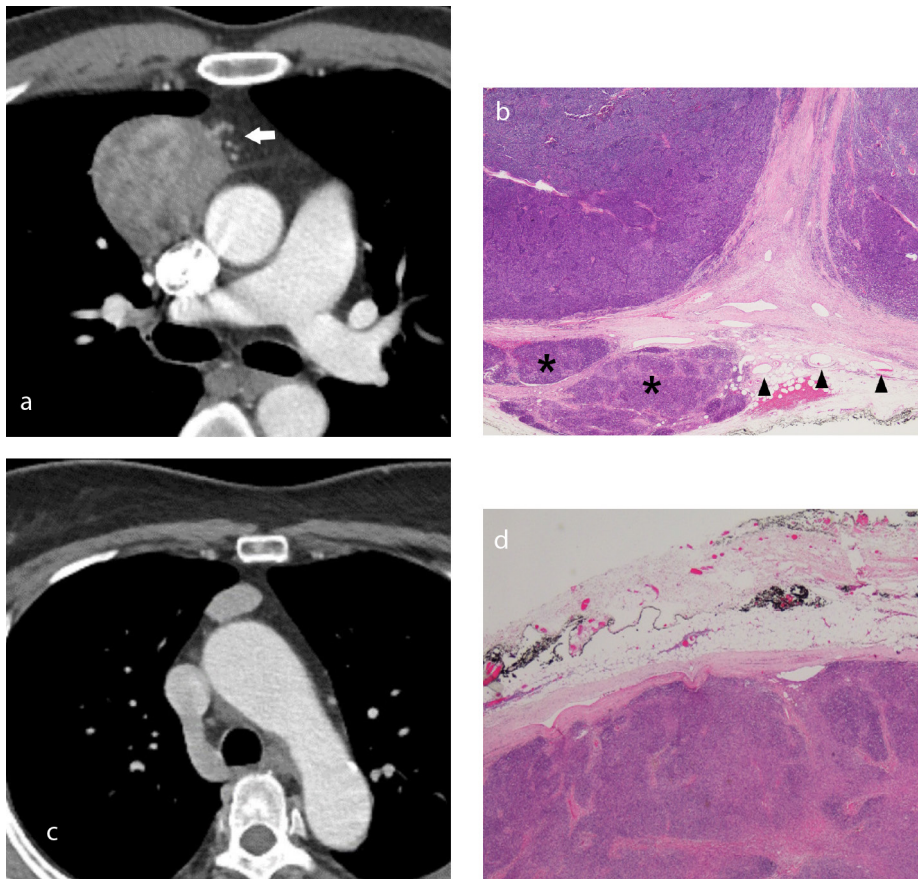
Figure 2. Representative cases of thymic epithelial tumors (TETs).

(a) Axial enhanced computed tomography (CT) image of a tumor measuring 7.1 cm, with a round shape, almost complete capsule integrity, and heterogeneous enhancement in the anterior mediastinum in a 48-year-old male patient. The tumor has measurable vascular structures around it (arrow), suggesting vascularity grade 2. **(b)** Example of a World Health Organization (WHO) type B1 and Masaoka–Koga stage II B TET. Thymoma with pericapsular invasion (asterisks), containing vessels in the pericapsular fat tissue (hematoxylin–eosin, original magnification ×20). **(c)** Axial enhanced CT image reveals a 2.6-cm oval-shaped mass with almost complete capsule integrity and homogeneous enhancement in the anterior mediastinum in a 58-year-old female patient. The tumor has no visible vascular structure around the TET, suggesting vascularity grade 0. **(d)** Example of a WHO type AB and Masaoka–Koga stage I TET. The TET is well encapsulated, without transcapsular or pericapsular invasion, and has no visible vessel in the pericapsular fat tissue (hematoxylin–eosin, original magnification ×20).

associated with transcapsular invasion in patients with TETs. Variables with $P < 0.20$ in the univariable analysis were included as input variables for the multivariable logistic regression analysis using the backward stepwise method. Goodness of fit for the logistic regression model was assessed using the Hosmer–Lemeshow and Omnibus tests. We also constructed a nomogram to predict the transcapsular invasion probability of a TET. Interobserver agreements for TETs on chest CT were assessed using Cohen's or weighted kappa coefficients. For all statistical analyses, the level of significance was set as $P < 0.05$. All statistical analyses were performed using SPSS statistical software (IBM, Armonk, NY, USA) and the R software package (version 4.0.3, The R Foundation for Statistical Computing).

Results

Clinical variables

The demographics of patients with TETs are listed in Table 1. A total of 116 patients, 52 (44.8%) men and 64 (55.2%) women and a mean age of 54.4 ± 12.3 years, were enrolled in the study. The patients were divided into a group without transcapsular invasion (n = 37) and a group with transcapsular invasion (n = 79) based on their pathology results. According to the WHO pathological classification, there were 5 (13.5%) patients with type A, 8 (21.6%) with type AB, 10 (27.0%) with type B1, 11 (29.7%) with type B2, 1 (2.7%) with type B3, and 2 (5.4%) with thymic carcinoma in the group without transcapsular invasion. There were 5 (6.3%) patients with type A, 9 (11.4%) with type AB, 19 (24.1%) with type B1, 19 (24.1%) with type B2, 9 (11.4%) with type B3, and 18 (22.8%)

Table 1. Clinical demographics and computed tomography image features of patients with thymic epithelial tumors

| Characteristic or findings | Total cohort (n = 116) | Masaoka–Koga stage | | P value |
		Group without transcapsular invasion (n = 37)	Group with transcapsular invasion (n = 79)	
Age†	54.4 ± 12.3	53.0 ± 12.7	55.0 ± 12.2	0.415
Sex				0.151
Male	52 (44.8%)	13 (35.1%)	39 (49.4%)	
Female	64 (55.2%)	24 (64.9%)	40 (50.6%)	
Myasthenia gravis				0.418
No	98 (84.5%)	33 (89.2%)	65 (82.3%)	
Yes	18 (15.5%)	4 (10.8%)	14 (17.7%)	
Size (cm)*	4.8 (2.8, 1.6–12.2)	4.3 (2.8, 1.9–9.5)	4.8 (2.6, 1.6–12.2)	0.438
Shape classification				<0.001
Round, oval	33 (28.4%)	19 (51.4%)	14 (17.7%)	
Lobular, irregular	83 (71.6%)	18 (48.6%)	65 (82.3%)	
Capsule integrity				<0.001
Almost complete	54 (46.6%)	27 (73.0%)	27 (34.2%)	
Partial complete	62 (53.4%)	10 (27.0%)	52 (65.8%)	
Calcification				0.467
No	96 (82.8%)	32 (86.5%)	64 (81.0%)	
Yes	20 (17.2%)	5 (13.5%)	15 (19.0%)	
Internal necrosis				0.380
No	95 (81.9%)	32 (86.5%)	63 (79.7%)	
Yes	21 (18.1%)	5 (13.5%)	16 (20.3%)	
Heterogenous enhancement				0.055
No	57 (49.1%)	23 (62.2%)	34 (43.0%)	
Yes	59 (50.9%)	14 (37.8%)	45 (57.0%)	
Pleural effusion				1.000
No	113 (97.4%)	36 (97.3%)	77 (97.5%)	
Yes	3 (2.6%)	1 (2.7%)	2 (2.5%)	
Pericardial effusion				1.000
No	111 (95.7%)	36 (97.3%)	75 (94.9%)	
Yes	5 (4.3%)	1 (2.7%)	4 (5.1%)	
Vascularity grade				<0.001
0	16 (13.8%)	11 (29.7%)	5 (6.3%)	
1	27 (23.3%)	14 (37.8%)	13 (16.5%)	
2	73 (62.9%)	12 (32.4%)	61 (77.2%)	
WHO				0.066
A	10 (8.6%)	5 (13.5%)	5 (6.3%)	
AB	17 (14.7%)	8 (21.6%)	9 (11.4%)	
B1	29 (25.0%)	10 (27.0%)	19 (24.1%)	
B2	30 (25.9%)	11 (29.7%)	19 (24.1%)	
B3	10 (8.6%)	1 (2.7%)	9 (11.4%)	
Carcinoma	20 (17.2%)	2 (5.4%)	18 (22.8%)	

† Variable is shown as mean ± standard deviation. *Variable is expressed with median, interquartile range, and range in parenthesis. Categorical variables are expressed as frequencies and percentage in parenthesis. WHO, World Health Organization.

with thymic carcinoma in the group with transcapsular invasion. There were no statistically significant differences in age, sex, or the presence of myasthenia gravis between the two groups ($P > 0.05$ for all).

Computed tomography image features

The TETs in the group with transcapsular invasion were more likely to have lobular or irregular shapes (65/79, 82.3%) than those in the group without (18/37, 48.6%) ($P < 0.001$). A significant difference was observed for capsule integrity ($P < 0.001$). The percentage of TETs with almost complete capsule integrity was higher in the group without transcapsular invasion (27/37, 73%) than in the group with transcapsular invasion (27/79, 34.2%). A significant difference was also observed for vascularity grade ($P < 0.001$). The percentage of TETs with vascularity grade 2 was higher in the group with transcapsular invasion (61/79, 77.2%) than in the group without (12/37, 32.4%). The median size of TETs was 4.3 (IQR = 2.8; range, 1.9–9.5) in the group without transcapsular invasion and 4.8 (IQR = 2.6; range, 1.6–12.2) in the group with transcapsular invasion ($P = 0.438$). Other CT image features, such as internal necrosis, heterogeneous enhancement, presence of calcification in the TET, pleural effusion, and pericardial effusion, were not significantly different between the two groups ($P > 0.05$ for all).

Interobserver agreement

Table 2 presents the interobserver agreement for the TET CT image evaluation of both observers. The shape classification yielded almost perfect agreement, with a Cohen's kappa value of 0.840 (95% CI: 0.761–0.893; $P < 0.001$). Capsule integrity yielded moderate agreement, with a Cohen's kappa value of 0.526 (95% CI: 0.292–0.682; $P < 0.001$). The vascularity grade indicated substantial agreement, with a weighted kappa value of 0.752 (95% CI: 0.662–0.841; $P < 0.001$). Other

variables (calcification, internal necrosis, and heterogeneous enhancement) also yielded almost perfect agreement (Cohen's kappa value > 0.9 for all; $P < 0.001$).

Univariable and multivariable analyses for transcapsular invasion

Table 3 lists the results of the univariable and multivariable analyses used to assess the association between transcapsular invasion and the clinical and radiological features on the preoperative chest CT in patients with TETs. The result of the Hosmer–Lemeshow test was $P = 0.681$ and that of the Omnibus test was $P < 0.001$, indicating that the logistic regression model had a good fit. In the univariable analysis, lobular or irregular shape (OR = 4.90; 95% CI: 2.09–11.90; $P < 0.001$), partial complete capsule integrity (OR = 5.20; 95% CI: 2.26–12.79; $P < 0.001$), and vascularity grade 2 (OR = 11.18; 95% CI: 3.44–41.35; $P < 0.001$) were significantly associated with transcapsular invasion. The variables of sex, shape, capsule integrity, heterogenous enhancement, and vascularity grade were included in the multivariable analysis using backward stepwise selection.

The multivariable analyses indicated that shape, capsule integrity, and vascularity grade were consistently associated with transcapsular invasion. A lobular or irregular shape had a 4.19 times higher risk (95% CI: 1.53–12.09; $P = 0.006$) than a round or oval shape of transcapsular invasion. In addition, partial complete capsule integrity had a 5.03 times higher risk (95% CI: 1.85–15.13; $P = 0.002$) than almost complete capsule integrity. Vascularity grade 2 had a 10.09 times higher risk (95% CI: 2.59–45.48; $P = 0.001$) than vascularity grade 0. Based on the multivariable logistic regression analysis, a graphical representation of a nomogram was constructed to predict transcapsular invasion in patients with TETs (Figure 3).

Discussion

The main results of our study revealed that shape classification, capsule integrity, and vascularity grade were independently associated with transcapsular invasion in patients with TETs. The interobserver agreements for shape classification, capsule integrity, and vascularity grade suggest that TET CT features have good reproducibility and help predict transcapsular invasion.

Based on the results, we assumed that vascularity grade reflects the degree of vascular proliferation in the anterior mediastinum. The vascular structures around the TETs were also confirmed in the pathological findings. Angiogenesis is indispensable for a tumor's growth.[20] Tomita et al.[21] demonstrated a significant correlation between tumor angiogenesis and invasiveness in patients with TETs. However, there are no studies on the growth of blood vessels around the TETs. The clinical implications of peritumoral vascularity on malignant tumors have been reported. In breast cancer, adjacent vessel signs, defined as the presence of peritumoral vessels that lead to a tumor, were significantly associated with the malignancy of a breast lesion and tumoral neovascularization; this finding was suggested as a possible explanation of the phenomenon. Additionally, adjacent vessel signs were significantly associated with malignancy and were observed more frequently in invasive cancers than in preinvasive cancers.[22,23] Zhang et al.[24] demonstrated that peritumoral vascularity was significantly associated with more aggressive subtypes of renal cell carcinoma. Therefore, the authors believe that peritumoral vascularity can represent the neovascularization of the tumor and may be associated with the invasiveness of TETs.

A few studies have reported interobserver agreements for shape, calcification, cystic or necrotic changes, enhancement

Table 2. Interobserver agreement for computed tomography features of thymic epithelial tumors

Variable	Agreement	Assessment
Shape classification	0.840 (0.761–0.893, $P < 0.001$)[a]	Almost perfect
Capsule integrity	0.526 (0.292–0.682, $P < 0.001$)[a]	Moderate
Calcification	0.984 (0.976–0.989, $P < 0.001$)[a]	Almost perfect
Internal necrosis	0.904 (0.856–0.935, $P < 0.001$)[a]	Almost perfect
Heterogeneous enhancement	0.913 (0.870–0.941, $P < 0.001$)[a]	Almost perfect
Vascularity grade	0.752 (0.662–0.841, $P < 0.001$)[b]	Substantial

[a]Cohen's Kappa value (95% confidence interval), [b]weighted Kappa value (95% confidence interval).

Table 3. Univariable and multivariable logistic regression analyses to assess the association between transcapsular invasion and clinical and radiological features on preoperative chest computed tomography in patients with thymic epithelial tumors

|	Univariable logistic regression analysis			Multivariable logistic regression analysis		
Characteristic or findings	OR	95% CI	*P* value	OR	95% CI	*P* value
Age	1.01	0.98, 1.05	0.412			
Sex*			0.153	Stepwise eliminated		
Male		Reference				
Female	1.80	0.81, 4.11				
Myasthenia gravis			0.343			
No		Reference				
Yes	1.78	0.58, 6.65				
Size, cm	1.07	0.9, 1.3	0.457			
Shape classification*			<0.001			
Round, oval		Reference			Reference	
Lobular, irregular	4.90	2.09, 11.9		4.19	1.53, 12.09	0.006
Capsule integrity*			<0.001			
Almost complete		Reference			Reference	
Partial complete	5.20	2.26, 12.79		5.03	1.85, 15.13	0.002
Calcification			0.469			
No		Reference				
Yes	1.50	0.53, 4.94				
Internal necrosis			0.383			
No		Reference				
Yes	1.63	0.58, 5.33				
Heterogenous enhancement			0.057	Stepwise eliminated		
No		Reference				
Yes	2.17	0.99, 4.93				
Pleural effusion			0.957			
No		Reference				
Yes	0.94	0.09, 20.51				
Pericardial effusion			0.566			
No		Reference				
Yes	1.92	0.27, 38.29				
Vascularity grade*						
0		Reference			Reference	
1	2.04	0.57, 7.99	0.281	1.41	0.31, 6.67	0.657
2	11.18	3.44, 41.35	<0.001	10.09	2.59, 45.48	0.001

OR, odds ratio; CI, confidence interval; *variables with *P* value <0.20 in the univariable analysis were included in the multivariable analysis.

patterns, enhancement degree, and the margin in TETs.[25,26] These findings are consistent with the results of the present study with the exception of shape classification. Although Yamazaki et al.[26] found that the interobserver agreement for shape classification demonstrated moderate agreement with a kappa value of 0.55, our interobserver agreement for shape classification yielded an almost perfect agreement, with a kappa value of 0.840. These differences are related to whether lobulated and irregular TET shapes were categorized in the same group when shape groups were classified. In the present study, classifying lobulated and irregular TET shapes in the same group was also associated with transcapsular invasion and yielded improved reproducibility.

Although additional validation is needed, the constructed nomogram can help predict transcapsular invasion in patients with TETs using preoperative chest CT. Complete thymectomy, which includes the complete removal of the thymus and surrounding mediastinal fat, is a standard method for treating TETs,[15,17] especially in patients at stage II or higher and those with concomitant myasthenia gravis. Thymomectomy, defined as the resection of the thymoma without perithymic tissue, is performed routinely on patients with TETs at Masaoka–Koga stage I. Thymomectomy is a less invasive procedure and is associated with a shorter operative time and hospitalization period.[27,28] Therefore, it is crucial to distinguish Masaoka–Koga stage I (no transcapsular invasion) from
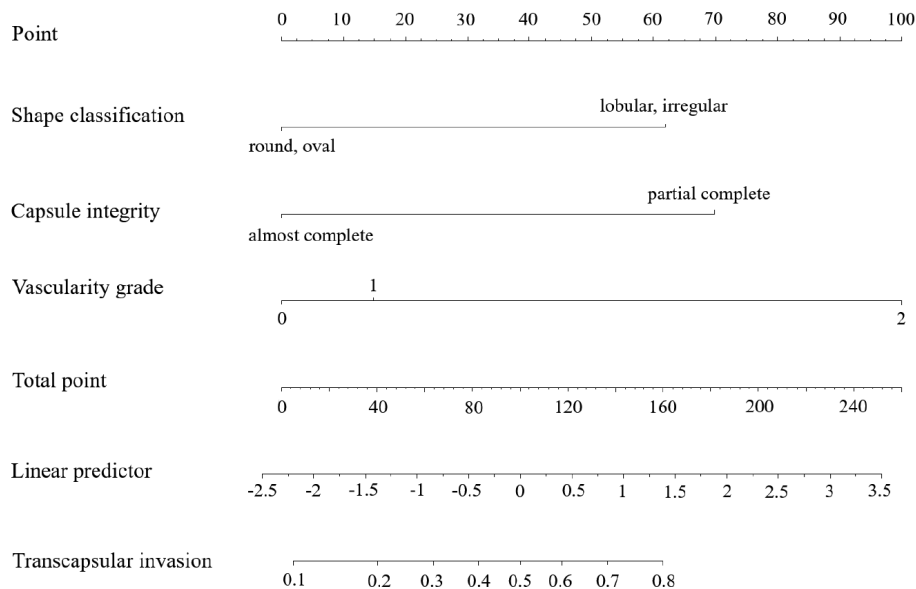
Figure 3. Nomogram to predict the likelihood of transcapsular invasion in patients with thymic epithelial tumors. The first row (point) is the point assignment for each computed tomography feature. Rows 2–4 represent the variables included in the model. The assigned points for three variables have been summed, and the total is shown in row 5 (total point). Once the total point is located, a vertical line is drawn between the fifth and final row (predicted probability of transcapsular invasion).

Masaoka–Koga stage II (or higher) in patients with TETs before surgery.

Our study has several limitations. First, this study was a retrospective analysis using clinical data from two institutions. Consequently, there may be an unintended selection bias. Second, we applied vascularity grade, which is a subjective, not quantitative, variable, in the prediction of the transcapsular invasion of TETs. We believe that the impact was minimal because the vascularity grades identified by the two experienced thoracic radiologists were in agreement. Third, we analyzed the CT features of TETs produced using various CT scanners with different CT protocols and contrast medium techniques, which could affect the CT features. However, we considered that the impact was minimal because the patients with poor CT image quality were excluded. We also assumed that the visual analysis of the TET CT images was minimally affected by the chest CT protocol, but additional research is needed on the qualitative analyses of TETs using CT images performed with standardized protocols. Finally, although vascularity grade reflects the extent of the peritumoral vascular structure, there is a lack of evidence to explain the association between peritumoral vascularity and tumor invasiveness. Therefore, an additional study is needed to clarify this association.

In conclusion, lobular or irregular shapes with partial complete capsule integrity and vascularity grade 2 exhibited good reproducibility outcomes and were independent predictors of transcapsular invasion on chest CT in patients with TETs. Therefore, the TET CT features of shape classification, capsule integrity, and vascularity grade can help identify transcapsular invasion in patients with TETs.

Conflict of interest disclosure

The authors declared no conflicts of interest.

References

1. Carter BW, Tomiyama N, Bhora FY, et al. A modern definition of mediastinal compartments. *J Thorac Oncol*. 2014;9(9 Suppl 2):97-101. [CrossRef]

2. de Jong WK, Blaauwgeers JL, Schaapveld M, Timens W, Klinkenberg TJ, Groen HJ. Thymic epithelial tumours: a population-based study of the incidence, diagnostic procedures and therapy. *Eur J Cancer*. 2008;44(1):123-130. [CrossRef]

3. Filosso PL, Ruffini E, Lausi PO, Lucchi M, Oliaro A, Detterbeck F. Historical perspectives: the evolution of the thymic epithelial tumors staging system. *Lung Cancer*. 2014;83(2):126-132. [CrossRef]

4. Masaoka A, Monden Y, Nakahara K, Tanioka T. Follow-up study of thymomas with special reference to their clinical stages. *Cancer*. 1981;48(11):2485-2492. [CrossRef]

5. Koga K, Matsuno Y, Noguchi M, et al. A review of 79 thymomas: modification of staging system and reappraisal of conventional division into invasive and non-invasive thymoma. *Pathol Int*. 1994;44(5):359-367. [CrossRef]

6. Jackson MW, Palma DA, Camidge DR, et al. The impact of postoperative radiotherapy for thymoma and thymic carcinoma. *J Thorac Oncol*. 2017;12(4):734-744. [CrossRef]

7. Detterbeck FC. Evaluation and treatment of stage I and II thymoma. *J Thorac Oncol*. 2010;5(10 Suppl 4):318-322. [CrossRef]

8. Roden AC, Yi ES, Jenkins SM, et al. Modified Masaoka stage and size are independent prognostic predictors in thymoma and modified Masaoka stage is superior to histopathologic classifications. *J Thorac Oncol*. 2015;10(4):691-700. [CrossRef]

9. Zhao Y, Chen H, Shi J, Fan L, Hu D, Zhao H. The correlation of morphological features of chest computed tomographic scans with clinical characteristics of thymoma. *Eur J Cardiothorac Surg*. 2015;48(5):698-704. [CrossRef]

10. Qu YJ, Liu GB, Shi HS, Liao MY, Yang GF, Tian ZX. Preoperative CT findings of thymoma are correlated with postoperative Masaoka clinical stage. *Acad Radiol*. 2013;20(1):66-72. [CrossRef]

11. Priola AM, Priola SM, Di Franco M, Cataldi A, Durando S, Fava C. Computed tomography and thymoma: distinctive findings in invasive and noninvasive thymoma and predictive features of recurrence. *Radiol Med*. 2010;115(1):1-21. [CrossRef]

12. Tomiyama N, Müller NL, Ellis SJ, et al. Invasive and noninvasive thymoma: distinctive CT features. *J Comput Assist Tomogr*. 2001;25(3):388-393. [CrossRef]

13. Marom EM, Milito MA, Moran CA, et al. Computed tomography findings predicting invasiveness of thymoma. *J Thorac Oncol*. 2011;6(7):1274-1281. [CrossRef]

14. Shen Y, Gu Z, Ye J, Mao T, Fang W, Chen W. CT staging and preoperative assessment of resectability for thymic epithelial tumors. *J Thorac Dis*. 2016;8(4):646-655. [CrossRef]

15. Gu Z, Fu J, Shen Y, et al. Thymectomy versus tumor resection for early-stage thymic malignancies: a Chinese Alliance for Research in Thymomas retrospective database analysis. *J Thorac Dis*. 2016;8(4):680-686. [CrossRef]

16. Onuki T, Ishikawa S, Iguchi K, et al. Limited thymectomy for stage I or II thymomas. *Lung Cancer*. 2010;68(3):460-465. [CrossRef]

17. Miller SJ. The National Comprehensive Cancer Network (NCCN) guidelines of care for nonmelanoma skin cancers. *Dermatol Surg*. 2000;26(3):289-292. [CrossRef]

18. Sadohara J, Fujimoto K, Müller NL, et al. Thymic epithelial tumors: comparison of CT and MR imaging findings of low-risk thymomas, high-risk thymomas, and thymic carcinomas. *Eur J Radiol*. 2006;60(1):70-79. [CrossRef]

19. Hu YC, Wu L, Yan LF, et al. Predicting subtypes of thymic epithelial tumors using CT: new perspective based on a comprehensive analysis of 216 patients. *Sci Rep*. 2014;4(1):6984. [CrossRef]

20. Viallard C, Larrivée B. Tumor angiogenesis and vascular normalization: alternative therapeutic targets. *Angiogenesis*. 2017;20(4):409-426. [CrossRef]

21. Tomita M, Matsuzaki Y, Edagawa M, et al. Correlation between tumor angiogenesis and invasiveness in thymic epithelial tumors. *J Thorac Cardiovasc Surg*. 2002;124(3):493-498. [CrossRef]

22. Dietzel M, Baltzer PA, Vag T, et al. The adjacent vessel sign on breast MRI: new data and a subgroup analysis for 1,084 histologically verified cases. *Korean J Radiol*. 2010;11(2):178-186. [CrossRef]

23. Fischer DR, Malich A, Wurdinger S, Boettcher J, Dietzel M, Kaiser WA. The adjacent vessel on dynamic contrast-enhanced breast MRI. *AJR Am J Roentgenol*. 2006;187(2):147-151. [CrossRef]

24. Zhang J, Lefkowitz RA, Wang L, et al. Significance of peritumoral vascularity on CT in evaluation of renal cortical tumor. *J Computer Assis Tomogr*. 2007;31(5):717-723. [CrossRef]

25. Chen X, Feng B, Li C, et al. A radiomics model to predict the invasiveness of thymic epithelial tumors based on contrast-enhanced computed tomography. *Oncol Rep*. 2020;43(4):1256-1266. [CrossRef]

26. Yamazaki M, Oyanagi K, Umezu H, et al. Quantitative 3D shape analysis of CT images of thymoma: a comparison with histological types. *AJR Am J Roentgenol*. 2020;214(2):341-347. [CrossRef]

27. Tseng YC, Hsieh CC, Huang HY S, et al. Is thymectomy necessary in nonmyasthenic patients with early thymoma? *J Thorac Oncol*. 2013;8(7):952-958. [CrossRef]

28. Nakagawa K, Yokoi K, Nakajima J, et al. Is thymomectomy alone appropriate for stage I (T1N0M0) thymoma? Results of a propensity-score analysis. *Ann Thorac Surg*. 2016;101(2):520-526. [CrossRef]